

Spectroscopic and Excited-State Properties of Tri-9-anthrylborane III: Crystal and Spectroscopic Polymorphisms

Eri Sakuda, Kiyoshi Tsuge, Yoichi Sasaki, and Noboru Kitamura*

Division of Chemistry, Graduate School of Science, Hokkaido University, Sapporo 060-0810, Japan

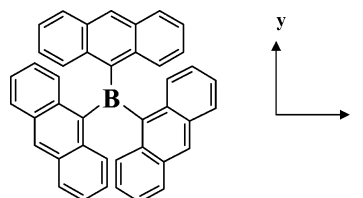
Received: August 15, 2005; In Final Form: September 29, 2005

We found that tri-9-anthrylborane (TAB) recrystallized from benzene produced both red cubic-like (R-form) and orange hexagon-like crystals (O-form). In both crystal forms, six TAB molecules are arranged in a honeycomb structure in the *ab* plane and benzene molecules are incorporated in the honeycomb structure, whose spatial geometry and the total number of benzene rings in the unit cell are different between the two forms: polymorphs with a different benzene content. In the R-form crystal, furthermore, interlayer stacking between left- and right-handed helical TAB molecules was observed in the *ac* plane, while each layer composed of stacked TAB molecules along the *c* axis was separated by benzene molecules in the O-form crystal, giving rise to more dense packing of TAB in the R-form crystal as compared to that in the O-form. Reflecting the crystal structures of the two forms, the charge transfer (CT) absorption and fluorescence spectra of the R-form crystal were shifted to the longer wavelength as compared to those in the O-form (i.e., crystal and spectroscopic polymorphisms) and, therefore, electronic interactions between TAB were stronger in the R-form as compared to those in the O-form. Furthermore, in addition to the main absorption ($\lambda_{\text{max}}^{\text{a}} = 499$ nm) and fluorescence peaks ($\lambda_{\text{max}}^{\text{f}} = 570$ nm), distinct absorption ($\lambda^{\text{a}} = \sim 470$ nm) and fluorescence bands ($\lambda^{\text{f}} = \sim 600$ nm) were observed for the R-form crystal, while the relevant absorption band in the O-form crystal ($\lambda^{\text{a}} = \sim 460$ nm) or in solution ($\lambda^{\text{a}} = \sim 435$ nm) was ambiguous. The results were discussed in terms of participation of the higher energy second CT transition in TAB.

Introduction

Triarylborane derivatives show very interesting electronic and spectroscopic properties.^{1–4} For example, tri-9-anthrylborane (TAB, see Chart 1) first reported by Yamaguchi et al. exhibits very unique spectroscopic properties in solution, featuring a characteristic absorption band at around λ (wavelength) = 470 nm (band I) in addition to a structured anthracene-like band at 330–400 nm (band II).² The compound also shows broad structureless fluorescence at around $\lambda = 510$ nm, which is different from that of anthracene itself; spectra are shown later. Our spectroscopic and theoretical studies on TAB demonstrated recently that the absorption band I originated from the charge transfer (CT) transition from the π -orbital of the anthryl group (abbreviated as $\pi(\text{An})$) to the vacant p-orbital on the boron atom (abbreviated as p(B)), while band II was attributed to the electronic transition to the π – π^* excited state of the anthryl group.^{3,4} The lowest singlet excited state of TAB is thus assigned to the CT state, and this accounts for broad and structureless fluorescence at $\lambda = 510$ nm. We also showed that the change in the electric dipole moment ($\Delta\mu$) accompanied by the electronic transition in band I was as large as ~ 8.0 D, as evaluated by solvent effects on the absorption/fluorescence spectra³ and the electroabsorption/electrofluorescence spectra of TAB in polymer films.⁴ Since 1,3,5-tri(9-anthryl)benzene does not show such spectroscopic characteristics and its absorption/fluorescence spectra are very similar to those of anthracene,⁵ the presence of p(B) in TAB provides extraordinary effects on the electronic and spectroscopic properties through the $\pi(\text{An})$ –p(B) interaction. Owing to such interesting charac-

CHART 1: Structure of Tri-9-anthrylborane (TAB)



teristics, triarylborane derivatives including their polymers have received current interest in both basic and applied (organic EL and LCD devices) research fields.^{2,6} However, experimental and theoretical studies on the spectroscopic/electronic properties of triarylborane derivatives are still limited, and fundamental knowledge about the derivatives is worth accumulating further in detail.

In the course of studying the spectroscopic and excited-state properties of TAB, we found that recrystallization of TAB from benzene produced simultaneously both red cubic-like (R-form) and orange hexagon-like crystals (O-form). Furthermore, the two crystals showed different absorption and fluorescence characteristics: structural, absorption, and fluorescence polymorphisms. These observations could provide new insight into detailed structural and spectroscopic characteristics of a triarylborane derivative. Although a large number of compounds are known to show a polymorphism,⁷ to the best of our knowledge, that of a triarylborane derivative has not been reported yet. In this paper, we report the structures of two polymorphic TAB crystals and their spectroscopic properties in the crystalline phase. Unique absorption and fluorescence spectra of the TAB crystals, different from those in solution,

* Address correspondence to this author. E-mail: kitamura@sci.hokudai.ac.jp.

were then discussed in terms of molecular packing of TAB in the crystals.

Experimental Section

X-ray Crystal Structure Analysis. TAB used in the present study was the same as that reported previously.³ The X-ray structural data of R- and O-form TAB crystals were collected on Mercury CCD area detectors coupled with Rigaku AFC-8S and AFC-7R diffractometers, respectively, by using CrystalClear (Rigaku Co.) with graphite-monochromated Mo K α radiation (0.7107 Å). The structures were solved by a Silicon Graphics O2 computer system by using teXsan, version 1.11 (Molecular Structure Co.). Full-matrix least-squares refinements were employed against F^2 . The crystallographic data (excluding structure factors) for the structure reported in this paper have been deposited with the Cambridge Crystallographic Data Centre as supplementary publication no. CCDC-170237. (Copies of the data can be obtained free of charge on application to CCDC, 12 Union Road, Cambridge CB2 1EZ, UK [fax (+44) 1223-336-033; e-mail deposit@ccdc.cam.ac.uk].)

Absorption and Fluorescence Spectroscopies. Absorption and fluorescence spectra of TAB in solution were recorded on a Hitachi U-3300 spectrophotometer and a Hitachi F-4500 spectrofluorometer, respectively. For absorption microspectroscopy, a Xe light beam being passed through a pinhole (diameter = 100 μ m) was introduced to an optical microscope (Optiphot-II, Nikon) and irradiated to single TAB crystals on a microscope stage through a microscope objective ($\times 100$, N.A. = 1.30). The Xe beam passed through a single TAB crystal was reflected by a half mirror set below the microscope stage and introduced to a multichannel-photodetector (PMA-11, Hamamatsu Photonics) through an optical fiber to record the absorption spectrum.⁸ For fluorescence microspectroscopy under aerated conditions, single TAB crystals were excited at 400 nm through the microscope objective lens by using the Xe lamp and a band-pass filter. The fluorescence from the crystal was collected by the same objective and detected with PMA-11.⁸ The absorption and fluorescence spectral band shapes of TAB were somewhat dependent on the size of the crystal, since irradiation of the crystal gave rise to complicated refraction/reflection of incident light and this disturbed more or less spectroscopic measurements. For absorption microspectroscopy, in particular, such a problem was serious. Therefore, we conducted repeated spectroscopic measurements for a number of TAB crystals with different sizes. The spectra reported here are the most reliable ones among the accumulated spectra.

Results and Discussion

Crystallographic Structures of Polymorphic TAB Crystals. The photographs of the red cubic-like and orange hexagonal-like TAB crystals (R- and O-form, respectively) obtained by recrystallization from benzene are shown in Figure 1a–c. Although we explored preparing polymorphic TAB crystals from other solvents (i.e., toluene, chloroform, and so forth), such crystals were not obtained other than those from benzene. When R- and O-form single crystals were dried in vacuo or under atmospheric pressure, the crystals were fractured very easily to the powders, indicating that benzene molecules were incorporated in the crystals as described later in detail. The present X-ray structure analysis was thus conducted immediately after collecting single TAB crystals from a benzene solution (see Figure 1a).

The crystal data for the two forms are summarized in Table 1. The atomic coordinates, bond lengths, bond angles, and other

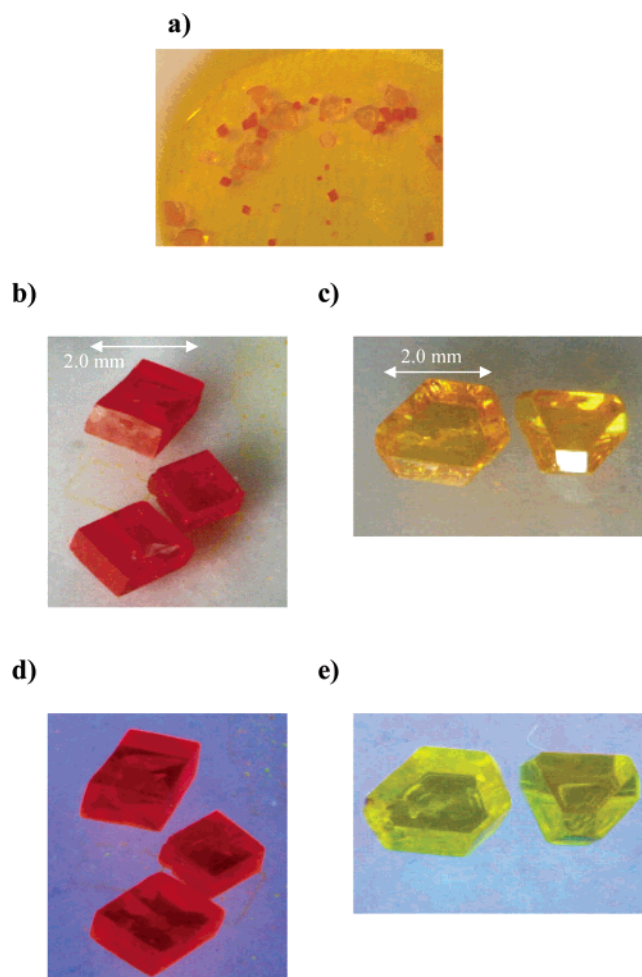


Figure 1. Photographs of TAB crystals: a mixture of the R- and O-form crystals precipitated in benzene (a); R- (b) and O-form crystals (c) under room light; and R- (d) and O-form crystals (e) under black-light (366 nm) illumination.

TABLE 1: Crystallographic Data for R- and O-Form TAB Crystals

crystal form	R-form	O-form
formula	C ₆₀ H ₄₅ B	C ₆₆ H ₅₁ B
fw	776.83	854.94
size, mm ³	0.75 \times 0.5 \times 0.25	0.65 \times 0.5 \times 0.5
<i>T</i> , K	153.1	213.1
cryst syst	trigonal	trigonal
space group	<i>R</i> 3	<i>R</i> 3c
cell constant		
<i>a</i> , Å	17.229(2)	15.9003(5)
<i>b</i> , Å	17.229(2)	15.9003(5)
<i>c</i> , Å	25.221(3)	66.652(3)
α , deg	90	90
β , deg	90	90
γ , deg	120	120
<i>V</i> , Å ³	6483(1)	14593.2(9)
<i>Z</i>	6	12
ρ_{calc} , g/cm ³	1.19	1.167
μ , mm ⁻¹	0.067	0.065
λ (Mo K α), Å	0.7107	0.7107
<i>R</i> 1%	0.0609	0.0646
w <i>R</i> 2%	0.1777	0.1841

$$R1 = \sum ||F_o| - |F_c|| / \sum |F_o|, wR2 = [\sum (|F_o| - |F_c|)^2 / \sum w|F_o|^2]^{1/2}.$$

structural parameters of the TAB crystals (see the Supporting Information, Tables S1–S6 and Figures S1 and S2) were very similar to those of the crystal obtained by recrystallization from *p*-xylene,² except for incorporation of benzene molecules in the present crystals. Since the main issue of the present study is to

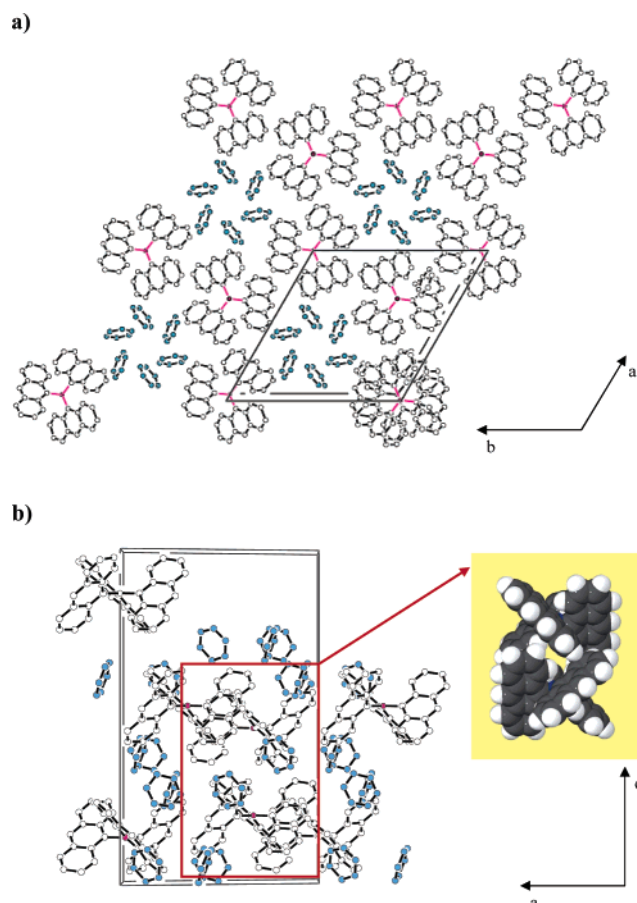


Figure 2. Crystal structure of the R-form crystal.

show structural and spectroscopic polymorphisms of TAB, we focus the following discussions on the molecular arrangements and packing of TAB in the two crystals.

The X-ray structures of the R- and O-form crystals are shown in Figures 2 and 3, respectively. As unique and common characteristics of both R- and O-form crystals, TAB molecules are arranged in a honeycomb manner in the *ab* plane (Figures 2a and 3a). Such an arrangement of TAB gives rise to the intermolecular nearest-neighbor distance between the anthryl groups being ~ 3.4 Å for both crystals. Although a face-to-face arrangement between two of any anthryl π -planes is not possible, the intermolecular distance of ~ 3.4 Å will be favorable for electronic interactions between TAB molecules. In the honeycomb structures produced by TAB, benzene molecules are incorporated in both R- and O-form crystals, while its spatial geometry is different between the two forms as seen in Figures 2 and 3, indicating TAB crystals show a polymorphism with a different solvent content. However, no TAB–benzene interaction is expected from their geometries and benzene acts as a space filler in the crystals. On the other hand, right-handed and left-handed helical TAB molecules stack with each other in the *ac* plane of the R-form crystal (Figure 2b), while each layer composed of stacked TAB molecules along the *c* axis is separated by benzene molecules in the O-form crystal (Figure 3b). The ratio of the number of the benzene molecule to that of TAB in a unit cell (TAB:benzene) in the R- or O-form crystal was 6:18 or 12:48, respectively. As a result, the interlayer distance in the R-form crystal is shorter (8.41 Å) than that in the O-form crystal (11.11 Å), indicating that intermolecular interactions between TAB would be stronger in the R-form as compared to those in the O-form. Furthermore, while the angle between the anthryl π -plane and the plane produced by the three

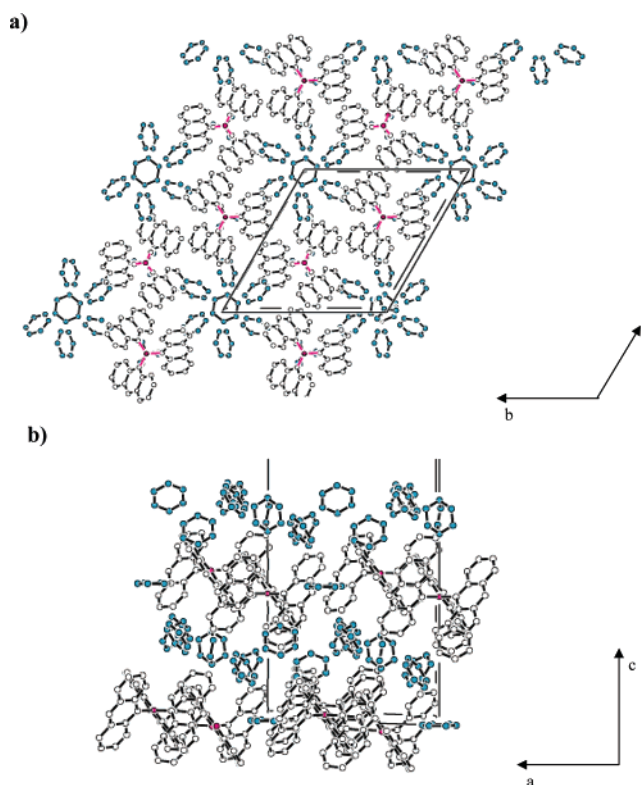


Figure 3. Crystal structure of the O-form crystal.

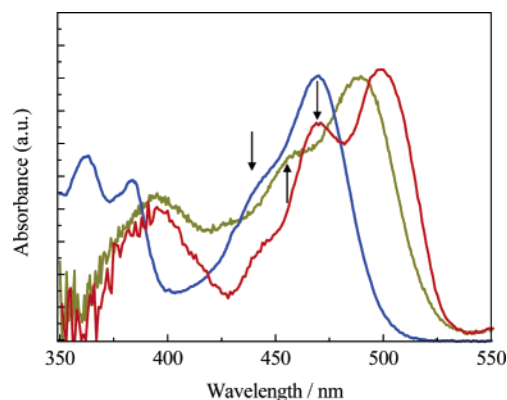


Figure 4. Absorption spectra of TAB in the R- (shown by red) and O-form crystals (orange), together with that in cyclohexane (blue).

boron–carbon bonds in TAB is estimated to be $\sim 57.3^\circ$ (AM1 calculations), that in the R- or O-form crystal has been determined to be 46.3° or 55.5° , respectively, demonstrating structural distortion of TAB in the crystalline phase.

Spectroscopic Polymorphisms of TAB Crystals. The differences in the molecular arrangements and packing of TAB between the R- and O-form crystals brought about the change in the crystal color. Besides the crystal color, furthermore, the R- and O-form crystals under illumination showed bright orange and yellow-orange fluorescence, respectively, although the photographs under illumination in panels d and e of Figure 1 were not necessarily clear enough. To obtain further detailed information about the characteristics of the crystals, we conducted absorption and fluorescence microspectroscopies of single R- and O-form crystals. The absorption and fluorescence spectra of the crystals are shown in Figures 4 and 5, respectively, together with those in cyclohexane for comparison. In cyclohexane, TAB showed the electronic transition to the π – π^* excited state in 330–400 nm (absorption band II) and that to the excited $\pi(\text{An})$ – $p(\text{B})$ CT state appeared at a maximum

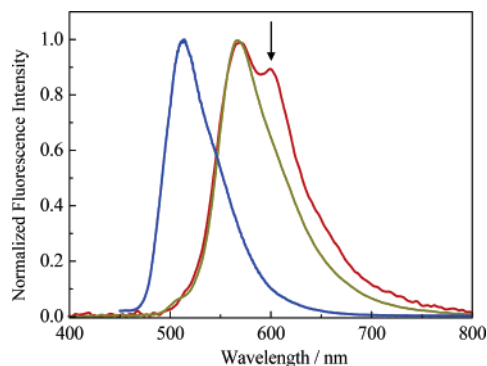


Figure 5. Fluorescence spectra of TAB in the R- (shown by red) and O-form crystals (orange), together with that in cyclohexane (blue). Excitation wavelength was 400 nm.

wavelength of $\lambda_{\max}^a = 470$ nm (band I), accompanying a weak shoulder at around $\lambda^a = 435$ nm.^{3,4} Both R- and O-form crystals showed analogous absorption spectra to that in cyclohexane. However, the absorption spectra of both R- and O-form crystals shifted to the longer wavelength by 20–30 nm as compared to that in cyclohexane; λ_{\max}^a of the CT band was 499 or 488 nm for the R- or O-form crystal, respectively. The results indicate stronger *intermolecular* electronic interactions between TAB molecules in the crystal as compared to those in solution.⁹ Structural distortion of TAB in the crystal, demonstrated by the angle between the anthryl π -plane and the plane produced by the three carbon–boron bonds described above, might also enhance *intramolecular* interactions between the anthryl groups in TAB through the change in π -conjugation via the p-orbital on the boron atom. Furthermore, the red-shifted spectrum of the R-form as compared to that of the O-form also demonstrates an electronic absorption polymorphism of the TAB crystals. Since TAB molecules in the R-form crystal are arranged more densely as compared to those in the O-form and intermolecular interactions between TAB are confirmed in both the *ab* and *ac* planes as described above, the red shift of the absorption spectrum of the R-form crystal relative to that of the O-form is the reasonable consequence. It is worth noting, furthermore, that the R-form crystal exhibits a clear absorption peak at $\lambda^a = \sim 470$ nm, while the relevant peak observed for the O-form crystal or in cyclohexane at $\lambda^a = \sim 460$ or 435 nm, respectively, is ambiguous and less-resolved: indicated by the arrows in Figure 4. These are the characteristic features of the absorption spectrum of TAB in the crystalline phase and are worth elucidating in detail: discussed later.

For both R- and O-form crystals, the fluorescence spectral band shape was similar to that in cyclohexane, while the maximum wavelength (λ_{\max}^f) of the O- or R-form shifted to the red by 54 (567 nm) or 57 nm (570 nm), respectively, as compared to that in cyclohexane (513 nm) (Figure 5). Although the difference in λ_{\max}^a between the R- and O-forms was 11 nm, λ_{\max}^f values of the two crystal forms were almost the same. This is not surprising, since excitation energy migration or hopping between the anthryl groups and/or TAB molecules should proceed very efficiently in the crystalline phase and the fluorescence process takes place from an energetically stable (i.e., low energy) trap site.¹⁰ In practice, although the fluorescence from TAB in solution showed a single-exponential decay,³ that in the crystal phase exhibited a multiexponential decay (data are not shown here), which supported efficient excitation energy migration/hopping in the crystal. Therefore, the fluorescence spectra of the crystals do not contradict with the relevant absorption spectrum in Figure 4. It is worth emphasizing, furthermore, that the R-form crystal shows a clear fluorescence

shoulder at $\lambda^f = \sim 600$ nm (shown by the arrow in Figure 5), while such a shoulder is not discernible in the O-form crystal or in cyclohexane, as far as the spectra in Figure 5 are concerned. An appearance of the fluorescence shoulder in the R-form is not fortuitous, but is highly reproducible. Furthermore, such fluorescence characteristics of the R-form crystal agreed very well with the observation of the well-resolved absorption peak at $\lambda^a = \sim 470$ nm. This is worth discussing in more detail to reveal the spectroscopic and electronic properties of TAB in the crystalline phase.

Absorption and Fluorescence Characteristics of TAB Crystals. The absorption and fluorescence spectra of the R-form crystal are characterized by the appearance of the distinct bands at around $\lambda^a = \sim 470$ and $\lambda^f = 600$ nm, respectively, in addition to the main peaks at $\lambda_{\max}^a = 499$ nm and $\lambda_{\max}^f = 570$ nm. A close inspection of the spectra in Figure 4 suggests that the absorption shoulder observed at $\lambda^a = 435$ nm in solution seems to relate with the peak at $\lambda^a = \sim 470$ or ~ 460 nm in the R- or O-form crystal, respectively. Therefore, the absorption shoulder of TAB at $\lambda^a = 435$ nm in solution is worth elucidating before discussing the spectroscopic characteristics of the TAB crystals.

The absorption shoulder of a triarylborane derivative similar to that of TAB in solution has been reported by Ramsey.¹ As an example, tri(*p*-tolyl)borane in methylcyclohexane exhibits an absorption shoulder at around $\lambda^a = 282$ nm in addition to the main absorption peak at $\lambda_{\max}^a = 297$ nm. Analogous spectroscopic characteristics also have been observed for triphenylborane ($\lambda_{\max}^a = 287$ nm and $\lambda^a = 276$ nm) and tri(1-naphthyl)borane ($\lambda_{\max}^a = 353$ nm and $\lambda^a = 287$ nm). Therefore, the observation of the absorption shoulder at around 435 nm for TAB in solution is not an experimental artifact and meaningful. According to Ramsey, the absorption shoulder observed for triarylborane is responsible for the second (high-energy) CT band, whose charge distribution in the excited state is different from that in the first CT excited state (i.e., low-energy main absorption band).¹ An analogous explanation to that for triphenylborane could be made for the absorption shoulder observed for TAB, since electroabsorption spectroscopy of TAB indicates that the electronic origin of the absorption band at $\lambda^a = 435$ nm is different from that at $\lambda_{\max}^a = 470$ nm (band I).⁴ As reported previously,^{4,11} when the electronic transition of a molecule accompanies the change in molecular polarizability (α) or electric dipole moment of the molecule ($\Delta\mu$), the relevant electroabsorption spectrum should be reproduced by the first or second derivative of the absorption spectrum, respectively. Therefore, the origin of an electronic absorption transition can be discussed by comparing the electroabsorption spectrum with the first or second derivative of the absorption spectrum. Figure 6 shows the absorption (top panel) and electroabsorption spectra of TAB (bottom panel, shown by the solid red curve) doped in a poly(methyl methacrylate) film (1.0%), together with the first and second derivatives of the absorption spectrum (middle panel, shown by the solid red and blue curves, respectively) and the simulated spectrum by the theoretical equations for electroabsorption (bottom panel, shown by the dotted red curve) (the data were taken from ref 4). As seen in Figure 6, while the lower energy electroabsorption spectrum corresponding to the main absorption band in 460–550 nm ($(18\text{--}21.5) \times 10^3 \text{ cm}^{-1}$) can be well reproduced by the second derivative of the absorption spectrum, that around the absorption shoulder (430–460 nm, $(21.5\text{--}23.0) \times 10^3 \text{ cm}^{-1}$) deviates from the second derivative, and the observed spectrum resembles rather the first derivative of the absorption spectrum. This demonstrates clearly that the origin

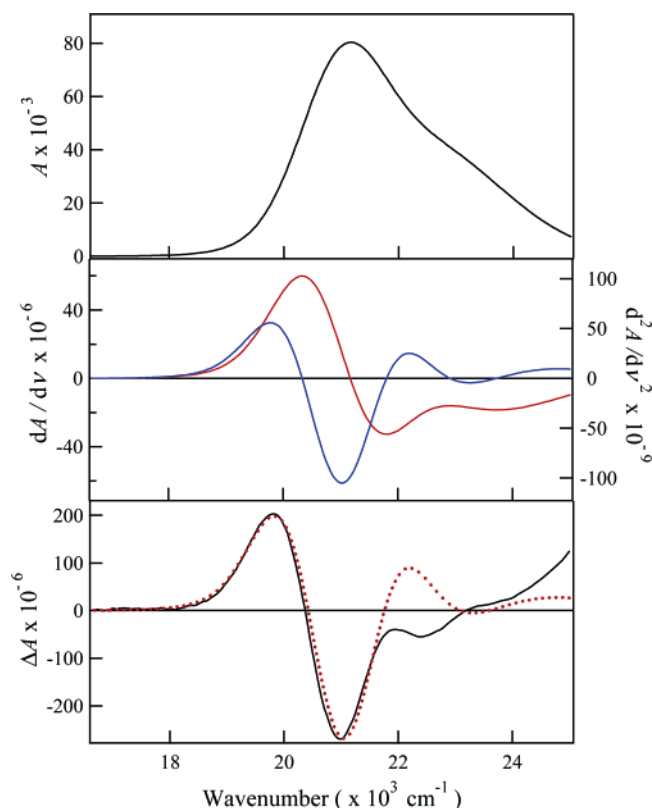


Figure 6. Absorption (top panel) and electroabsorption spectra (bottom panel, shown by black) of TAB doped in poly(methyl methacrylate) films. The middle panel shows the first (red) and second derivatives of the absorption spectrum (blue). The red-dotted spectrum in the bottom panel represents the simulated curve. Data taken from ref 4; the experimental details have been reported therein.

of the electronic transition observed at around 435 nm is different from that of the main absorption peak (470 nm), indicating that the absorption shoulder observed for TAB is best explained by the second CT transition. Owing to the similarities of the absorption spectrum of TAB in solution with those in the crystals, therefore, we conclude that the absorption band observed for the R- or O-form crystal at $\lambda^a = \sim 470$ or ~ 460 nm, respectively, is also responsible for the second CT transition, whose charge distribution in the excited state is different from that in the first CT excited state.

Our previous studies on TAB demonstrated that the molar absorptivity (ϵ) of the CT band I was dependent on a solvent and the results were explained in terms of the change in the degree of $\pi(\text{An})$ – $p(\text{B})$ mixing (i.e., HOMO–LUMO interaction) through variation of the conformation of TAB with a solvent.³ Analogous discussions also have been reported by Ramsey for several triarylborane derivatives.¹ In the crystalline phase, the degree of $\pi(\text{An})$ – $p(\text{B})$ mixing will be dependent on the crystal structure. In the R-form crystal, TAB molecules are stacked between the *ac* layers (Figure 2b) and this makes the angle between the anthryl π -plane and the plane produced by the three carbon–boron bonds 46.3° , while that in the O-form crystal is 55.5° as discussed before. Therefore, the R-form crystal is structurally distorted as compared to the O-form crystal or TAB in solution. Such a structural distortion of TAB in the crystalline phase would give rise to more or less the change in the degree of $\pi(\text{An})$ – $p(\text{B})$ mixing and, therefore, the absorption strength (ϵ). The relatively strong and distinct absorption peak observed at $\lambda^a = \sim 470$ nm in the R-form crystal as compared to that in solution or the O-form crystal thus would be due to the increase

in the degree of $\pi(\text{An})$ – $p(\text{B})$ mixing for the second CT transition.

On the other hand, optical excitation (400 nm) of the absorption band I produces both the first and second CT excited states. However, since very fast internal conversion should take place from the higher energy second CT excited state to the lowest CT excited state, the fluorescence bands observed for the R-form crystal at 570 and 600 nm should be ascribed to the fluorescence from the first CT excited state. In the crystalline phase, excitation energy migration/hopping proceeds very efficiently and an energetically stable trap site(s) emits fluorescence. Because of interlayer stacking between TAB molecules in the R-form crystal, the crystal would possess at least two energetically stable trap sites, which emit fluorescence independently at 570 and 600 nm.

Conclusions

It was demonstrated that R-form and O-form TAB crystals exhibited quite interesting properties. The present study indicates that the symmetrical structure of TAB is the key for determining both crystal structures and electronic/spectroscopic properties. Because of D_3 symmetry in the ground state, TAB molecules are arranged in a honeycomb structure in the crystal. Although both R- and O-form crystals were characterized by honeycomb arrangements of TAB molecules, the inclusion mode of benzene inside the honeycomb structure produced by six TAB molecules and the layer-by-layer structure were different between the two crystals, leading to the structural polymorphism with a different benzene content. Furthermore, interlayer stacking between right-handed and left-handed helical TAB molecules in the R-form crystal brought about more dense packing of TAB and, thus, stronger intermolecular interactions between TAB as compared to those in the O-form crystal, as shown clearly by absorption and fluorescence microspectroscopies. Furthermore, this reflected on the characteristic absorption and fluorescence spectra of the R-form crystal, showing intense bands at around 470 and 600 nm, respectively, in addition to the main absorption (495 nm) and fluorescence bands (570 nm). The absorption characteristics of the R-form crystal were explained reasonably by the electronic transitions to both the first (495 nm) and second CT excited states (470 nm), while the fluorescence bands at 570 and 600 nm were discussed in terms of excitation energy migration/hopping to different trap sites. The unique spectroscopic characteristics of the R-form crystal were shown to be responsible for the interlayer stacking of TAB molecules in the crystal.

Acknowledgment. N.K. thanks a Grant-in-Aid for Scientific Research from the Ministry of Education, Culture, Sports, Science and Technology of the Japanese Government (MEXT) for support of the research (No. 13853004).

Supporting Information Available: X-ray crystallographic files for the R- and O-form TAB crystals (Tables S1–S6 and Figures S1 and S2). This material is available free of charge via the Internet at <http://pubs.acs.org>.

References and Notes

- (1) (a) Ramsey, B. G.; El-Bayoumi, M.; Kasha, M. *J. Phys. Chem.* **1961**, 65, 1502. (b) Ramsey, B. G.; Leffler, J. E. *J. Phys. Chem.* **1963**, 67, 2242. (c) Ramsey, B. G. *J. Phys. Chem.* **1966**, 70, 611. (d) Miller, D. S.; Leffler, J. E. *J. Phys. Chem.* **1970**, 74, 2571.
- (2) Yamaguchi, S.; Akiyama, S.; Tamao, K. *J. Am. Chem. Soc.* **2000**, 122, 6335.
- (3) Kitamura, N.; Sakuda, E. *J. Phys. Chem. A* **2005**, 109, 7429.

- (4) Kitamura, N.; Sakuda, E.; Yoshizawa, T.; Iimori, T.; Ohta, N. *J. Phys. Chem. A* **2005**, *109*, 7435.
- (5) Kitamura, N.; Iwahashi, Y.; Sakuda, E.; Ishizaka, S. Unpublished results.
- (6) (a) Yamaguchi, S.; Shirasaka, T.; Tamao, K. *Org. Lett.* **2000**, *2*, 4129. (b) Yamaguchi, S.; Akiyama, S.; Tamao, K. *J. Am. Chem. Soc.* **2001**, *123*, 11372. (c) Yamaguchi, S.; Akiyama, S.; Tamao, K. *J. Orgmet. Chem.* **2002**, *652*, 3. (d) Yamaguchi, S.; Shirasaka, T.; Akiyama, S.; Tamao, K. *J. Am. Chem. Soc.* **2002**, *124*, 8816. (e) Yuan, Z.; Taylor, N. J.; Marder, T. B.; Williams, I. D.; Kurtz, S. K.; Cheng, L.-T. *J. Chem. Soc., Chem. Commun.* **1990**, 1489. (f) Yuan, Z.; Taylor, N. J.; Sun, Y.; Marder, T. B.; Williams, I. D.; Cheng, L.-T. *J. Organomet. Chem.* **1993**, *449*, 27. (g) Yuan, Z.; Taylor, N. J.; Ramachandran, R.; Marder, T. B. *Appl. Organomet. Chem.* **1996**, *10*, 305. (h) Yuan, Z.; Collings, J. C.; Taylor, N. T.; Marder, T. B.; Jardin, C.; Halet, J. F. *J. Solid State Chem.* **2000**, *154*, 5. (i) Lee, B. Y.; Wang, S.; Putzer, M.; Bartholomew, G. P.; Bu, X.; Bazan, G. C. *J. Am. Chem. Soc.* **2000**, *122*, 3969. (j) Lee, B. Y.; Bazan, G. C. *J. Am. Chem. Soc.* **2000**, *122*, 8577. (k) Matsumi, N.; Naka, K.; Chujo, Y. *J. Am. Chem. Soc.* **1998**, *120*, 5112. (l) Matsumi, N.; Naka, K.; Chujo, Y. *J. Am. Chem. Soc.* **1998**, *120*, 10776. (m) Noda, T.; Shirota, Y. *J. Am. Chem. Soc.* **1998**, *120*, 9714. (n) Noda, T.; Ogawa, H.; Shirota, Y. *Adv. Mater.* **1999**, *11*, 283.
- (7) Sarma, J. A. R. P.; Desiraju, G. R. *Crystal Engineering*; Seddon, K. R., Zaworotko, M., Eds.; Kluwer Publishing: Norwell, MA, 1999.
- (8) Nakatani, K.; Chikama, K.; Kitamura, N. *Adv. Photochem.* **1999**, *25*.
- (9) In absorption microspectroscopy, since the transmittance of the microscope optics decreases sharply at $\lambda < 400$ nm, the absorption spectra of the crystals at $\lambda < 400$ nm cannot be compared directly with that in cyclohexane. However, the diffuse reflectance absorption spectrum of the R or O crystal showed a red shift (~ 20 nm) and broadening of the $\pi-\pi^*$ band ($\lambda = 350-400$ nm) as compared to that in cyclohexane. This indicates stronger electronic interactions between TAB/anthryl groups in the crystals.
- (10) Birks, J. B. *Photophysics of Aromatic Molecules*; Wiley-Interscience: London, UK, 1970.
- (11) (a) Ohta, N. *Bull. Chem. Soc. Jpn.* **2002**, *75*, 1637. (b) Ponder, M.; Mathies, R. J. *J. Phys. Chem.* **1983**, *87*, 5090. (c) Oh, D. H.; Sano, M.; Boxer, S. G. *J. Am. Chem. Soc.* **1991**, *113*, 6880.